Available online at www.sciencedirect.com
SCIENCE DIRECT®
Comput. Methods Appl. Mech. Engrg. 194 (2005) 1385–1404
Computer methods in applied mechanics and engineering
www.elsevier.com/locate/cma

Flexibility-based upper bounds on the response variability of simple beams

Vissarion Papadopoulos [a,*], George Deodatis [b], Manolis Papadrakakis [a]

[a] Institute of Structural Analysis and Seismic Research, National Technical University, Athens 15780, Greece
[b] Department of Civil Engineering and Engineering Mechanics, Columbia University, New York, NY 10027, USA

Received 25 September 2003; received in revised form 10 April 2004; accepted 22 June 2004

Abstract

Spectral- and probability-distribution-free upper bounds on the response variability of both statically determinate and indeterminate beams are established in the present paper based on exact closed-form analytic expressions derived for the variance of the response displacement. A conjecture has to be made in the case of statically indeterminate beams in order to establish these bounds. The conjecture is supported through an argument postulating the existence of an integral form for the variance of the response displacement and through a brute-force optimization procedure providing numerical validation. Such bounds require knowledge of only the variance of the stochastic field modeling the inverse of the elastic modulus and are realizable in the sense that it is possible to fully determine the probabilistic characteristics of the stochastic field (modeling the inverse of the elastic modulus) that produces them. Furthermore, it is possible to fully determine also the corresponding stochastic field modeling the elastic modulus that produces these bounds. These spectral- and probability-distribution-free bounds can also be computed numerically using a so-called fast Monte Carlo simulation procedure that does not require a closed-form analytic expression for the response displacement, making this approach much more general. Numerical examples are provided involving a statically determinate and a statically indeterminate beam.

Keywords: Upper bounds; Stochastic fields; Stochastic finite element analysis; Variability response function; Monte Carlo simulation; Optimization

* Corresponding author.
E-mail addresses: vpapado@central.ntua.gr (V. Papadopoulos), deodatis@civil.columbia.edu (G. Deodatis), mpapadra@central.ntua.gr (M. Papadrakakis).

0045-7825/$ - see front matter © 2004 Published by Elsevier B.V.
doi:10.1016/j.cma.2004.06.040

1. Introduction

The analysis of stochastic systems with material/geometric properties modelled by random fields has been the subject of extensive research in the past two decades. Over these years, very few analytic solutions have been established, mainly for simple linear elastic structures under static loads. Meanwhile, the majority of the work has focused on developing Stochastic Finite Element Methodologies (SFEM) for the numerical solution of the stochastic differential equations involved in the problem. By far, the most widely used SFEM approaches are approximate expansion/perturbation based methods. Although such methods have proven to be highly accurate and computationally efficient for a wide range of problems, there are still several classes of problems in stochastic mechanics involving combinations of strong nonlinearities, large variations of system properties and non-Gaussian system properties that can be solved with reasonable accuracy only through a computationally expensive Monte Carlo simulation approach.

Whether an expansion/perturbation based approach or a Monte Carlo simulation methodology is used to estimate the response variability of a stochastic system, it is necessary to know the marginal probability distribution function (pdf) and the spectral/correlation characteristics of the stochastic system properties. Unfortunately, in most practical engineering applications, there is a lack of experimental data that would enable a quantification of such probabilistic characteristics of the stochastic system properties. Taking into account that many researchers have clearly demonstrated that both the correlation structure and the marginal pdf of the material/geometric properties can have a significant (and in certain cases dramatic) effect on the stochastic response, a SFEM or Monte Carlo analysis will not provide particularly useful results for real-life applications when the probabilistic characteristics of the system properties are arbitrarily assumed. Actually, there is no way to check in such a case whether the results will be conservative or unconservative with respect to structural safety without performing an extensive (and in most cases computationally prohibitive) sensitivity analysis. The aforementioned observations demonstrate clearly the importance of establishing spectral- and probability-distribution-free upper bounds on the response variability of stochastic systems. In order for such bounds to be useful for practical applications, they must be *realizable*, in the sense that it should be possible to determine the specific probabilistic characteristics of the random system properties that produce them.

The first attempt to establish spectral-distribution-free upper bounds on the response variability of stochastic systems goes back to the 1980s. Shinozuka [9] introduced the concept of the Variability Response Function, which makes possible the establishment of such bounds using only the coefficient of variation (variance) of the stochastic field describing the material/geometric properties. As described in [9], the variance of the response displacement u can be expressed in the following integral form:

$$\mathrm{Var}[u] = \int_{-\infty}^{\infty} \mathrm{VRF}(\kappa) S_{ff}(\kappa)\, \mathrm{d}\kappa, \tag{0a}$$

where the variability response function (VRF) is a function depending only on deterministic parameters related to the geometry, material properties and loading of the structure, S_{ff} is the spectral density function of the stochastic field modeling the material/geometric properties, and κ is the wave number. An upper bound for the variance of u can then be easily established as

$$\mathrm{Var}[u] \leqslant \mathrm{VRF}(\kappa^{\max})\sigma_{ff}^2 \tag{0b}$$

with $\kappa^{\max}$ being the wave number where the VRF attains its maximum value and σ_{ff}^2 being the variance of the stochastic field modeling the material/geometric properties. Furthermore, Eq. (0a) indicates that the VRF provides insight into the mechanisms controlling the response variability of stochastic systems.

It should be noted, however, that the derivation of the VRF in Eq. (0a) (refer to [9] for the detailed derivation) was based on a first-order approximation of the inverse of the stochastic field modeling the spatial variability of the elastic modulus. Such an approximation leads to spectral-distribution-free upper bounds estimated through Eq. (0b) that are reasonably accurate only for relatively small values of the coefficient of variation of the elastic modulus (generally less than 20%). In [9], the VRF was determined analytically for simple linear elastic and statically determinate beams under static loads. Later on, Deodatis and Shinozuka extended the VRF concept into the framework of a finite element formulation for the case of statically determinate and indeterminate frame structures [2,3]. In these two papers, the VRF was expressed in closed form in terms of products of matrices and vectors. Eventually, expressions for the VRF were established for plane stress/strain problems, plate bending problems, as well as for systems with multiple correlated random properties [6,7,10].

A common drawback of all the aforementioned extensions of the VRF is that a first-order approximation of some kind (usually of the response displacement) is used for their derivation. An immediate consequence is that even the existence of the integral form in Eq. (0a) depends on this approximation. As a fast Monte Carlo technique is developed later to estimate numerically the VRF through Eq. (0a), the existence of the integral form in Eq. (0a) has to be conjectured in the general case (when no first-order approximation is considered). This was recognized in a series of two papers by Deodatis et al. [4,5], where it was shown that the bounds obtained from Eq. (0b) can be exceeded when using certain stochastic fields with bimodal marginal pdf's to model the material properties, even for relatively small coefficients of variation of these properties (less than 20%). In these two papers, new spectral- and probability-distribution-free upper bounds on the response variability were proposed, based on the coefficient of variation (variance) and lower limit of the elastic modulus. It was conjectured that these new upper bounds were produced by so-called "associated fields" obtained by mapping random sinusoids—having a symmetric U-shaped beta marginal pdf—to fields with a generally non-symmetric U-shaped beta marginal pdf with lower limit equal to the lower limit of the elastic modulus. It should be noted that the upper bounds established earlier in [9,2,3,6,7,10] are produced by random sinusoids reflecting only the coefficient of variation of the elastic modulus. Although the conjecture made in [4,5] for the new upper bounds was supported by a semi-analytical demonstration, as well as by extensive numerical evidence, further improvement is certainly possible in the estimation of the bounds as the problem of the transition from the inverse of the elastic modulus to the elastic modulus itself was not fully addressed in [4,5].

The present paper therefore attempts for the first time to deal with this transition problem in a direct way by establishing exact expressions for the response variability based on the inverse of the elastic modulus. These exact expressions lead to the evaluation of realizable upper bounds on the response variance of statically determinate and indeterminate beams using the variance of the inverse of their elastic modulus. A conjecture has to be made in the case of statically indeterminate beams in order to establish the bounds. Two important conclusions are eventually drawn: (i) the response variability is bounded under certain conditions, with upper bounds that are realizable in the sense that they correspond to a stochastic field that can be fully determined, and (ii) the upper bounds are indirectly related to the variability of the elastic modulus, since by nature these bounds are directly related to the variability of the inverse of the elastic modulus. It is this second feature of the response variability that is responsible for some of the limitations of previous efforts, as they all tried to connect the response variability directly to the variability of the elastic modulus, an approach that involves always some level of approximation. Consequently, it is believed that the upper bounds proposed in this study constitute an improvement over the earlier ones. It should be mentioned at this juncture that the approach of modeling the beam flexibility instead of its rigidity has already been followed in a small number of earlier studies (e.g. [11]). In these studies, exact expressions for the response variance were established for simple statically determinate beams under static loading (but not upper bounds).

The upper bounds established in this study for the response variability are spectral- and probability-distribution-free requiring knowledge of only the variance of the inverse of the elastic modulus. It should be mentioned that the variance of the inverse of the elastic modulus can be obtained as easily as the variance of the elastic modulus using the same experimental data. The proposed bounds are realizable in the sense that it is possible to determine the probabilistic characteristics (spectral density function and marginal probability distribution function) of the stochastic field (modeling the inverse of the elastic modulus) that produces them. Furthermore, it is possible to fully determine also the corresponding stochastic field modeling the elastic modulus that produces these bounds.

2. Statically determinate beam

Consider the statically determinate cantilever beam of length L shown in Fig. 1, with a uniformly distributed load Q_0 and a concentrated moment M_0 imposed at the free end. The loads are assumed to be static and deterministic. The inverse of the elastic modulus of the beam is assumed to vary randomly along its length according to the following expression:

$$\frac{1}{E(x)} = F_0(1 + f(x)), \tag{1}$$

where E is the elastic modulus, F_0 is the mean value of the inverse of E, and $f(x)$ is a zero-mean homogeneous stochastic field modeling the variation of $1/E$ around its mean value F_0.

The response displacement of the beam $u(x)$ is given by

$$u(x) = -\frac{F_0}{I}\int_0^x (x-\xi)M(\xi)(1+f(\xi))\,\mathrm{d}\xi = -\frac{F_0}{I}\int_0^x h(x,\xi)M(\xi)(1+f(\xi))\,\mathrm{d}\xi, \tag{2}$$

where $h(x,\xi)$ is the Green function of the beam, I is the moment of inertia, and $M(x)$ is the bending moment function given by

$$M(x) = -\frac{Q_0}{2}(L-x)^2 + M_0. \tag{3}$$

Using Eq. (2), the mean of $u(x)$ is expressed as

$$\varepsilon[u(x)] = -\frac{F_0}{I}\int_0^x h(x,\xi)M(\xi)\varepsilon[(1+f(\xi))]\,\mathrm{d}\xi \tag{4}$$

and the mean square as

$$\varepsilon[u^2(x)] = \frac{F_0^2}{I^2}\int_0^x\int_0^x h(x,\xi_1)h(x,\xi_2)M(\xi_1)M(\xi_2)\varepsilon[(1+f(\xi_1))(1+f(\xi_2))]\,\mathrm{d}\xi_1\,\mathrm{d}\xi_2. \tag{5}$$

The response variance is then determined from Eqs. (4) and (5) as follows:

$$\mathrm{Var}[u(x)] = \varepsilon[u^2(x)] - \varepsilon[u(x)]^2 = \frac{F_0^2}{I^2}\int_0^x\int_0^x h(x,\xi_1)h(x,\xi_2)M(\xi_1)M(\xi_2)R_{ff}(\xi_1-\xi_2)\,\mathrm{d}\xi_1\,\mathrm{d}\xi_2, \tag{6}$$

where $R_{ff}(\xi_1 - \xi_2)$ denotes the autocorrelation function of stochastic field $f(x)$.

Applying the Wiener–Khintchine transform to the autocorrelation function in Eq. (6), the variance of the response displacement can be written as

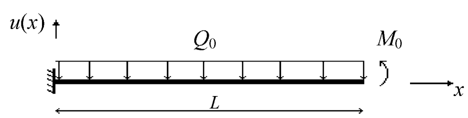

Fig. 1. Configuration of statically determinate beam.

$$\mathrm{Var}[u(x)] = \int_{-\infty}^{\infty} \mathrm{VRF}(x,\kappa) S_{ff}(\kappa)\,\mathrm{d}\kappa, \tag{7}$$

where the variability response function (VRF) is given by

$$\mathrm{VRF}(x,\kappa) = \left| \frac{F_0}{I} \int_0^x h(x,\xi) M(\xi) \mathrm{e}^{i\kappa\xi}\,\mathrm{d}\xi \right|^2 \tag{8}$$

and $S_{ff}(\kappa)$ denotes the power spectral density function of stochastic field $f(x)$. The above expressions for the $\mathrm{Var}[u(x)]$ and the VRF (Eqs. (7) and (8) respectively) are *exact analytic expressions*, since no approximations were made for their derivation. In addition, the VRF expression in Eq. (8) is a general one that can be applied to any statically determinate beam with any kind of boundary or loading conditions, using the appropriate Green and bending moment functions.

Since both $S_{ff}(\kappa)$ and $\mathrm{VRF}(x,\kappa)$ are even functions of κ, the variance of $u(x)$ can also be written as

$$\mathrm{Var}[u(x)] = 2\int_0^{\infty} \mathrm{VRF}(x,\kappa) S_{ff}(\kappa)\,\mathrm{d}\kappa. \tag{9}$$

Taking advantage of the integral form of Eq. (9), upper bounds on the response displacement variance can be established as follows:

$$\mathrm{Var}[u(x)] = 2\int_0^{\infty} \mathrm{VRF}(x,\kappa) S_{ff}(\kappa)\,\mathrm{d}\kappa \leqslant \mathrm{VRF}(x,\kappa^{\max})\sigma_{ff}^2, \tag{10}$$

where $\kappa^{\max}$ is the wave number at which the VRF takes its maximum value, and σ_{ff}^2 is the variance of stochastic field $f(x)$.

The upper bound given in Eq. (10) is physically realizable since the form of stochastic field $f(x)$ that produces it is known. Specifically, the variance of $u(x)$ attains its upper bound value of $\mathrm{VRF}(x,\kappa^{\max})\sigma_{ff}^2$ when random field $f(x)$ becomes a random sinusoid, i.e.

$$f(x) = \sqrt{2}\sigma_{ff}\cos(\kappa^{\max}x + \varphi). \tag{11}$$

In Eq. (11), φ is a random phase angle uniformly distributed in the range $[0, 2\pi]$. In this case, the corresponding spectral density function of $f(x)$ is a delta function at wave number $\kappa^{\max}$

$$S_{ff}(\kappa) = \sigma_{ff}^2\delta(\kappa - \kappa^{\max}), \tag{12}$$

while its marginal pdf is a beta probability distribution function given by

$$p_f(s) = \frac{1}{\pi\sqrt{2\sigma_{ff}^2 - s^2}} \quad \text{with } -\sqrt{2}\sigma_{ff} \leqslant s \leqslant \sqrt{2}\sigma_{ff}. \tag{13}$$

The upper bound provided in Eq. (10) is spectral- and probability-distribution-free, since the only probabilistic parameter it depends on is the standard deviation of the inverse of the elastic modulus.

The exact expressions for the $\mathrm{Var}[u(x)]$ and the VRF in Eqs. (7) and (8) are identical to the corresponding classic (but approximate) expressions established in [1] and [9], except of one notable difference in Eq. (7). Specifically, in Eq. (7), $S_{ff}(\kappa)$ is now the spectral density function of stochastic field $f(x)$ modeling the inverse of the elastic modulus, while in the classic approximate formulation ([1,9]), $f(x)$ models the elastic modulus. Consequently, the exact VRF in Eq. (8) preserves the basic characteristic of the classical one in the sense that it depends only on deterministic parameters describing the geometry, material properties and loading of the structure.

3. Statically indeterminate beam

Consider now the statically indeterminate beam of length L shown in Fig. 2, with a deterministic uniformly distributed load Q_0 The inverse of the elastic modulus is again assumed to vary randomly along the length of the beam according to Eq. (1).

Using a force (flexibility) method formulation, the response displacement of this beam $u(x)$ can be expressed as

$$u(x) = u_0(x) - Ru_1(x), \tag{14}$$

where $u_0(x)$ is the deflection of the associated statically determinate beam with uniform load Q_0 obtained by removing the simple support at the right end of the beam in Fig. 2, $u_1(x)$ is the deflection of the same associated statically determinate beam due to a unit concentrated force acting at $x = L$, and R is the redundant force (vertical reaction at the right end of the beam in Fig. 2).

Eq. (14) is then written as follows:

$$\begin{aligned} u(x) &= \frac{F_0 Q_0}{2I}\int_0^x (x-\xi)(L-\xi)^2(1+f(\xi))\,\mathrm{d}\xi - \frac{F_0 R}{I}\int_0^x (x-\xi)(L-\xi)(1+f(\xi))\,\mathrm{d}\xi \\ &= \int_0^x g_1(x,\xi)(1+f(\xi))\,\mathrm{d}\xi + \int_0^x g_2(x,\xi)R(1+f(\xi))\,\mathrm{d}\xi \end{aligned} \tag{15a}$$

where

$$g_1(x,\xi) = \frac{F_0 Q_0}{2I}(x-\xi)(L-\xi)^2 \quad \text{and} \quad g_2(x,\xi) = -\frac{F_0}{I}(x-\xi)(L-\xi). \tag{15b}$$

The redundant force R is a random variable that can be computed from the boundary condition at $x = L$ as

$$u(x=L) = 0 \Rightarrow u_0(x=L) = Ru_1(x=L) \Rightarrow R = \frac{\dfrac{Q_0}{2}\displaystyle\int_0^L (L-\xi)^3(1+f(\xi))\,\mathrm{d}\xi}{\displaystyle\int_0^L (L-\xi)^2(1+f(\xi))\,\mathrm{d}\xi} \tag{16}$$

For the trivial case where stochastic field $f(x)$ degenerates into a random variable, Eq. (16) indicates that the redundant force R reduces to a deterministic variable. Consequently, the VRF of the statically indeterminate beam reduces to the expression given in Eq. (8) for the statically determinate beam. The statically determinate beam for this case is the associated statically determinate beam loaded with the uniform load Q_0 and an additional deterministic concentrated force at the right end equal to R.

For the general case where $f(x)$ is a stochastic field, taking the expectation on both sides of Eq. (15a), the mean value of $u(x)$ is computed as follows:

$$\varepsilon[u(x)] = \int_0^x g_1(x,\xi)\,\mathrm{d}\xi + \int_0^x g_2(x,\xi)\varepsilon[R(1+f(\xi))]\,\mathrm{d}\xi, \tag{17}$$

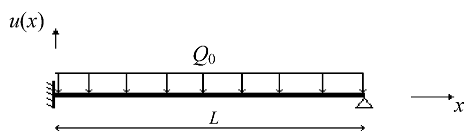

Fig. 2. Configuration of statically indeterminate beam.

Combining now Eqs. (15a) and (17), the following expression is written for $u(x) - \varepsilon[u(x)]$

$$u(x) - \varepsilon[u(x)] = \int_0^x \{g_1(x,\xi)(1+f(\xi)) + g_2(x,\xi)R(1+f(\xi)) - g_1(x,\xi) - g_2(x,\xi)\varepsilon[R(1+f(\xi))]\}\,\mathrm{d}\xi$$
$$= \int_0^x \{g_1(x,\xi)f(\xi) + g_2(x,\xi)p(\xi)\}\,\mathrm{d}\xi, \tag{18}$$

where

$$p(x) = R(1+f(x)) - \varepsilon[R(1+f(x))] \tag{19}$$

can be easily shown to be a zero-mean, non-homogeneous stochastic field. The variance of the response displacement $u(x)$ is then computed as

$$\mathrm{Var}[u(x)] = \varepsilon\{(u(x) - \varepsilon[u(x)])^2\}$$
$$= \int_0^x \int_0^x \{g_1(x,\xi_1)g_1(x,\xi_2)R_{ff}(\xi_1 - \xi_2) + g_2(x,\xi_1)g_2(x,\xi_2)R_{pp}(\xi_1,\xi_2)$$
$$+ g_1(x,\xi_1)g_2(x,\xi_2)\varepsilon[f(\xi_1)p(\xi_2)] + g_1(x,\xi_2)g_2(x,\xi_1)\varepsilon[p(\xi_1)f(\xi_2)]\}\,\mathrm{d}\xi_1\,\mathrm{d}\xi_2, \tag{20}$$

where $R_{pp}(\xi_1,\xi_2)$ denotes the autocorrelation function of stochastic field $p(x)$. The quantities $\varepsilon\,[f(\xi_1)p(\xi_2)]$ and $\varepsilon[p(\xi_1)f(\xi_2)]$ in Eq. (20) are the cross-correlation functions $R_{fp}(\xi_1,\xi_2)$ and $R_{pf}(\xi_1,\xi_2)$ of stochastic fields $f(x)$ and $p(x)$. Since by definition $R_{pf}(\xi_1,\xi_2) = R_{fp}(\xi_2,\xi_1)$, Eq. (20) can be rewritten as follows:

$$\mathrm{Var}[u(x)] = \int_0^x \int_0^x \{g_1(x,\xi_1)g_1(x,\xi_2)R_{ff}(\xi_1 - \xi_2) + g_2(x,\xi_1)g_2(x,\xi_2)R_{pp}(\xi_1,\xi_2)$$
$$+ 2g_1(x,\xi_1)g_2(x,\xi_2)R_{fp}(\xi_1,\xi_2)\}\,\mathrm{d}\xi_1\,\mathrm{d}\xi_2. \tag{21}$$

The expression in Eq. (21) is an *exact expression* for the variance of the displacement $u(x)$ of the statically indeterminate beam in Fig. 2. In addition, it is a general expression that can be applied to any statically indeterminate beam with the same boundary conditions, using the appropriate Green and bending moment functions depending on the loading conditions of the beam, while similar expressions can be derived in a straightforward manner for different boundary conditions, including more than one redundant reactions. The response variance can therefore be calculated directly using Eq. (21) without the need of resorting to a brute-force Monte Carlo simulation or to a SFEM approach. It should be mentioned here that a brute-force Monte Carlo simulation approach involves the generation of a large number of sample functions of stochastic field $f(x)$, subsequent (deterministic) numerical solution of the resulting beams with the generated fluctuations of the inverse of the elastic modulus, and eventual estimation of $\mathrm{Var}[u(x)]$ from the resulting beam responses. Going back to Eq. (21), in order to determine $\mathrm{Var}[u(x)]$, it is necessary to know the autocorrelation function $R_{pp}(\xi_1,\xi_2)$ and the cross-correlation function $R_{fp}(\xi_1,\xi_2)$. It appears to be quite difficult to establish analytic expressions for these two functions. However, numerical estimations of these two functions are straightforward through the following simulation approach: generate a sample function of stochastic field $f(x)$, calculate R using Eq. (16), determine $p(x)$ through Eq. (19), and estimate $R_{pp}(\xi_1,\xi_2)$ and $R_{fp}(\xi_1,\xi_2)$ using a large number of such sample realizations.

Fig. 3 displays results from the calculation of $\mathrm{Var}[u(x)]$ using brute-force Monte Carlo simulation versus application of Eq. (21) as described in the previous paragraph. The structure considered is the statically indeterminate beam of Fig. 2 and the stochastic field $f(x)$ is assumed to have the power spectrum $S_{ff}(\kappa)$ defined in Eq. (12). The following values are used for the mean value of the inverse of the elastic modulus, the uniform load, the length of the beam, its moment of inertia, and the standard deviation of the inverse of the elastic modulus: $F_0 = 8 \times 10^{-9}$ m^2/N, $Q_0 = 1{,}000$ N/m, $L = 10$ m, $I = 0.1$ m^4 and $\sigma_{ff} = 0.40$. In Fig. 3, $\mathrm{Var}[u(x = L/2)]_\kappa$ is plotted as a function of the wave number κ indicating the location where all the power of $f(x)$ is located (refer to $\kappa^{\max}$ in Eq. (12)). In other words, each value of κ used for the evaluation of $\mathrm{Var}[u(x = L/2)]_\kappa$ in Fig. 3 corresponds to a different power spectrum $S_{ff}(\kappa)$ as defined in Eq. (12). From

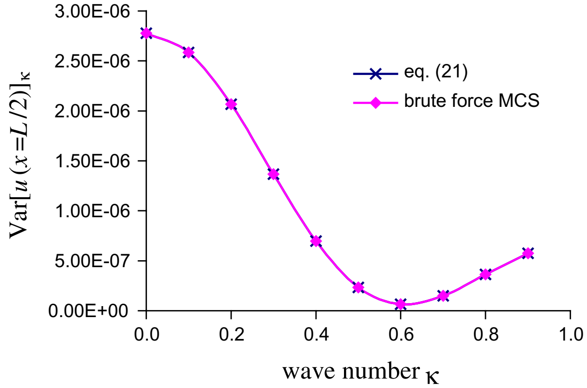

Fig. 3. Variance of response displacement at midspan for the statically indeterminate beam in Fig. 2, having the inverse of the elastic modulus described by a stochastic field with power spectrum as in Eq. (12) (random sinusoid). $\mathrm{Var}[u(x = L/2)]_\kappa$ is computed using Eq. (21) and brute-force Monte Carlo simulation. κ is the wave number where the random sinusoid has all its power concentrated (compare to $\kappa^{\max}$ in Eq. (12)).

Fig. 3, it can be easily observed that the results obtained using Eq. (21) practically coincide with those obtained from the brute-force Monte Carlo simulation approach.

In order to be able to establish upper bounds on the response variability of statically indeterminate beams, an integral expression for the response variance similar to that in Eqs. (7) and (9) has to be established from Eq. (21). This appears to be a particularly challenging task because of the presence of $R_{pp}(\xi_1,\xi_2)$ and $R_{fp}(\xi_1,\xi_2)$ in Eq. (21) involving the non-homogeneous field $p(x)$ that is obtained from stochastic field $f(x)$ through the nonlinear transformation shown in Eq. (19).

For the purposes of this study, therefore, the *existence* of an integral expression of the following form:

$$\mathrm{Var}[u(x)] = 2\int_0^\infty \mathrm{VRF}(x,\kappa)S_{ff}(\kappa)\,\mathrm{d}\kappa \tag{22}$$

is conjectured for the response displacement variance of the statically indeterminate structure, although a closed-form analytic expression for the variability response function $\mathrm{VRF}(x,\kappa)$ is not available.

The main argument in support of the aforementioned conjecture is described in the following. From the definition of stochastic field $p(x)$ in Eq. (19), it appears that its correlation structure has a lot of similarities with that of $f(x)$ (consider for this purpose a sample function of $f(x)$ and the corresponding sample function of $p(x)$ obtained through Eqs. (16) and (19)). It should be therefore possible to express the non-homogeneous auto- and cross-correlation functions $R_{pp}(\xi_1,\xi_2)$ and $R_{fp}(\xi_1,\xi_2)$ as a function (admittedly unknown) of the homogeneous auto-correlation function $R_{ff}(\xi_1-\xi_2)$. Then $R_{ff}(\xi_1-\xi_2)$ becomes a common factor of all three terms in the integrand in Eq. (21), and the integral expression of Eq. (22) follows in a straightforward way. Additional evidence about the validity of this conjecture will be provided later in this study through numerical experimentation involving a Monte Carlo simulation based approach to numerically estimate $\mathrm{VRF}(x,\kappa)$ and an optimization algorithm.

3.1. Numerical evaluation of VRF(x,κ) and establishment of upper bounds for the response displacement variance of the statically indeterminate beam

After making the conjecture postulating the existence of the integral form for $\mathrm{Var}[u(x)]$ shown in Eq. (23), it is necessary to find a methodology to numerically evaluate the functional form of $\mathrm{VRF}(x,\kappa)$. For this purpose, the computationally efficient fast Monte Carlo simulation (FMCS) approach (e.g. [5]) will be used. The basic steps of this approach are described in the following.

1. Generate N sample functions of a random sinusoid with standard deviation σ_{ff} and wave number $\bar{\kappa}$ modeling the inverse of the elastic modulus
$$f_j(x) = \sqrt{2}\sigma_{ff}\cos(\bar{\kappa}x + \phi_j); \quad j = 1, 2, \ldots, N, \tag{23}$$
where ϕ_j are random phase angles uniformly distributed in the range $[0, 2\pi]$.
2. Using these N generated sample functions of $f_j(x)$ for a specific value of $\bar{\kappa}$ and the exact analytic deterministic expression for the response displacement of the statically indeterminate beam (Eq. (15)), it is straightforward to compute the corresponding N displacement responses. Then, the variance of the response $\mathrm{Var}[u(x)]_{\bar{\kappa}}$ can be easily estimated numerically for a specific value of $\bar{\kappa}$ by ensemble averaging the N computed responses.
3. The value of the VRF of the statically indeterminate beam at wave number $\bar{\kappa}$ is then computed from:
$$\mathrm{VRF}(x, \bar{\kappa}) = \frac{\mathrm{Var}[u(x)]_{\bar{\kappa}}}{\sigma_{ff}^2} \tag{24}$$
4. Steps 1–3 are repeated for different values of the wave number $\bar{\kappa}$ of the random sinusoid and the $\mathrm{VRF}(x,\kappa)$ is computed over a wide range of wave numbers, wave number by wave number.

Eq. (24) is a direct consequence of Eq. (22), when the stochastic field $f(x)$ modeling the inverse of the elastic modulus becomes a random sinusoid.

Finally, the maximum value of $\mathrm{VRF}(x,\kappa)$ multiplied by σ_{ff}^2 determines the upper bound on the variance of the response displacement, exactly in the same way as for the statically determinate beam (Eq. (10)). The specific value of the wave number where this maximum value occurs (denoted by $\kappa^{\max}$) completely determines the stochastic field (a random sinusoid in this case) that produces the upper bound (realizable upper bounds).

A note is in order at this point regarding the generation of random phase angles in Eq. (23). It has been suggested [5] that in order to reduce the computational effort, the N random phase angles ϕ_j should be selected to be equally spaced in the range $[0, 2\pi]$. Although in general the value of N required for convergence varies depending on both the problem under consideration and the specific value of the wave number $\bar{\kappa}$, convergence is usually observed for values of N as low as 10, making this Monte Carlo simulation procedure very efficient computationally. The reader is referred to [5] for more details. This is the reason the methodology is called "Fast Monte Carlo Simulation".

Although for the case of statically determinate beams the variability response function can be computed from the closed-form analytic expression shown in Eq. (8), it should be mentioned that, alternatively, the $\mathrm{VRF}(x, \kappa)$ can also be estimated using the fast Monte Carlo simulation approach described above. This could prove to be helpful in cases where Green's function of the statically determinate problem becomes too cumbersome. The only difference from the statically indeterminate case in such a computation is that no conjecture is now needed for establishing the integral form in Eq. (9).

3.2. Brute-force optimization procedure in support of the conjecture made for Eq. (22)

As mentioned previously, the establishment of upper bounds for the case of statically indeterminate beams is based on the conjecture of existence of an integral expression for $\mathrm{Var}[u(x)]$ of the form shown in Eq. (22). Following this conjecture, the bounds can be computed using Eq. (10), after the $\mathrm{VRF}(x, \kappa)$ is estimated using the fast Monte Carlo simulation approach described in the previous section.

In this section, a brute-force optimization procedure will be followed to numerically validate this conjecture. Specifically, the upper bound for Var[$u(x)$] estimated using Eq. (10), in conjunction with fast Monte Carlo simulation to compute the VRF(x, κ), will be compared to the corresponding upper bound obtained through a brute-force optimization procedure. This optimization scheme starts with the computation of Var[$u(x)$] using a stochastic field $f(x)$ with arbitrarily defined power spectrum and marginal pdf (the computation of Var[$u(x)$] involves the generation of a large number of sample functions of stochastic field $f(x)$, subsequent (deterministic) numerical solution of the resulting beams with the generated fluctuations of the inverse of the elastic modulus, and eventual estimation of Var[$u(x)$] from the resulting beam responses). Proceeding from this initial stochastic field $f(x)$, the optimization scheme estimates through an iterative algorithm the form of stochastic field $f(x)$ that maximizes Var[$u(x)$]. It is obvious that such a brute-force optimization procedure is totally independent of the conjecture of existence of an integral expression for Var[$u(x)$] of the form shown in Eq. (22). It is shown that the two upper bounds obtained from the two different approaches coincide, and that the stochastic fields that produce this common upper bound are identical random sinusoids.

The brute-force iterative optimization procedure is described in the following in relation to the statically indeterminate beam shown in Fig. 2. The inverse of the elastic modulus is considered to vary randomly along the length of the beam according to Eq. (1). The initial assumption for stochastic field $f(x)$ involves a power spectrum that decreases linearly from $S_{ff}^{(0)}(\kappa = 0) = 0.0457$ to $S_{ff}^{(0)}(\kappa = 3.5) = 0.0$, and a marginal pdf initially assumed to be a truncated Gaussian within the following limits: $-0.9 \leqslant f(x) \leqslant 0.9$ (to avoid non-positive values of the inverse of the elastic modulus). The standard deviation of $f(x)$ is $\sigma_{ff} = 0.4$. The spectral representation method is used to simulate the zero-mean, homogeneous, truncated-Gaussian, stochastic field $f(x)$. The optimization procedure followed has many similarities to the one used in [8]. Its various steps are described below.

(1) *Iteration 0*. Using the initial assumption for the power spectrum $S_{ff}^{(0)}(\kappa)$ of stochastic field $f(x)$ modeling the inverse of the elastic modulus, NSIM Gaussian sample functions of $f(x)$ are generated using the spectral representation method. If any of these generated sample functions have values outside the range $-0.9 \leqslant f(x) \leqslant 0.9$, then these values are set equal to the corresponding limit they exceed (either -0.9 or 0.9). It should be mentioned here that the aforementioned truncation will modify the power spectrum of the generated sample functions. However, this is not creating any problem, as the ultimate objective here is to determine where is the iterative algorithm converging to and not to accurately reflect the initial power spectrum. Using these NSIM generated sample functions of stochastic field $f(x)$, the corresponding NSIM displacement responses of the statically indeterminate beam in Fig. 2 are computed using the exact expression in Eq. (15). The following values are used for the various parameters describing the problem: $F_0 = 8 \times 10^{-9}\,\mathrm{m}^2/\mathrm{N}$, $L = 10\,\mathrm{m}$, and $I = 0.1\,\mathrm{m}^4$. Then, the variance of the response displacement at the 0th iteration (denoted by Var$^{(0)}$) is computed through ensemble averaging of the NSIM computed displacement responses.

(2) *Iteration m*. Select randomly two entries of the power spectrum at iteration $(m-1)S_{ff}^{(m-1)}(\kappa_j);\ j = 1, 2$, and modify their values by $\Delta S_{ff}(\kappa_j)$ so that a new power spectrum is created for iteration $(m) : S_{ff}^{(m)}(\kappa_j) = S_{ff}^{(m-1)}(\kappa_j) + \Delta S_{ff}(\kappa_j);\ j = 1, 2$. The rest of the entries of the power spectrum at iteration $(m-1)$ remain unchanged. The selection of these two entries is done with equal probability for all entries. In order for the new spectrum at iteration (m) to have the same variance with the spectrum at iteration $(m-1)$, the two modification values $\Delta S_{ff}(\kappa_j)$; $j = 1, 2$ must satisfy the following condition:

$$\Delta S_{ff}(\kappa_1) = -\Delta S_{ff}(\kappa_2). \tag{25}$$

The selected values of $\Delta S_{ff}(\kappa_j)$; $j = 1, 2$ have to be such that the values of the new spectrum at iteration (m) at wave numbers κ_1 and κ_2 remain non-negative. Using the new spectrum at iteration (m), NSIM sample functions of the truncated stochastic field $f(x)$ are then generated via the spectral representation method. The corresponding NSIM displacement responses are computed using the exact expression in Eq. (15), and eventually used to estimate the variance of the response displacement at the mth iteration (denoted by $\mathrm{Var}^{(m)}$).

(3) If $\mathrm{Var}^{(m-1)} < \mathrm{Var}^{(m)}$ the modifications to the power spectrum are accepted. Otherwise, they are rejected.

(4) Set $m = m + 1$ and go back to step 3.

The iterations are stopped when a significant number of iterations go without producing a further increase in the variance of the response displacement. It is pointed out again that the maximum value for the variance of the response displacement obtained through this optimization procedure is not making use of the conjecture of existence of an integral expression for $\mathrm{Var}[u(x)]$ of the form shown in Eq. (22).

Two load cases are considered in relation to the statically indeterminate beam in Fig. 2. The first load case (LC1) is the one presented in Fig. 2 with a uniformly distributed load $Q_0 = 1000\,\mathrm{N/m}$, while the second load case (LC2) adds a concentrated moment $M_0 = -10{,}000\,\mathrm{Nm}$ at its right end (please note that this concentrated moment is not indicated in Fig. 2).

Fig. 4 presents results of the aforementioned optimization procedure for the displacement at the midpoint ($x = L/2$) of the beam in Fig. 2 and LC1. The evolution of the power spectrum $S_{ff}^{(m)}(\kappa)$ is presented

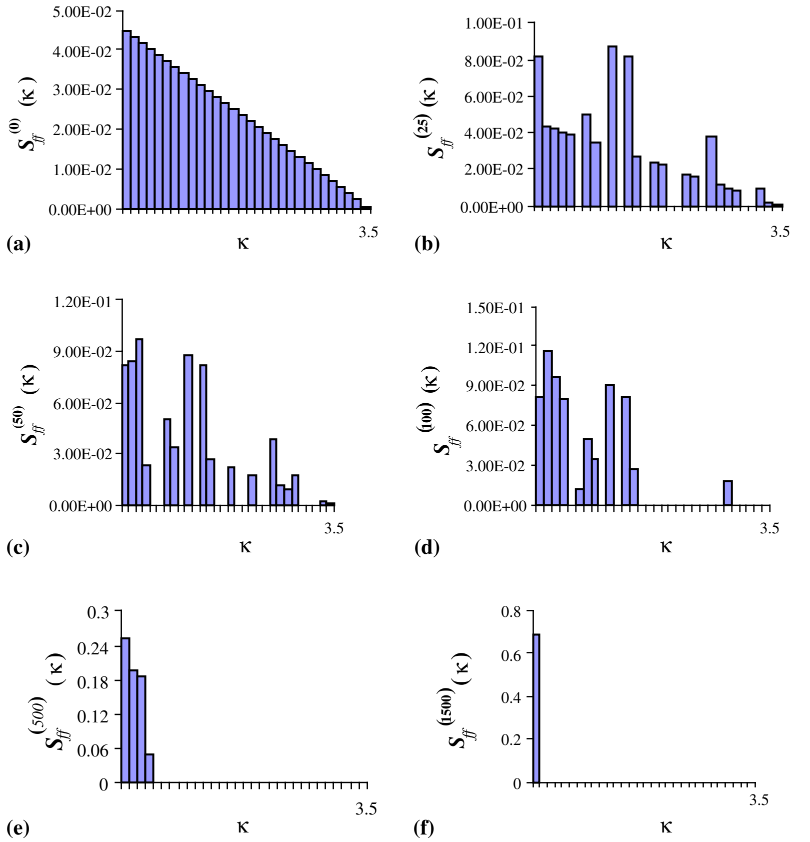

Fig. 4. Evolution of power spectrum of $f(x)$ during the optimization procedure to estimate the maximum variance of the midpoint displacement of the beam in Fig. 2 with LC1.

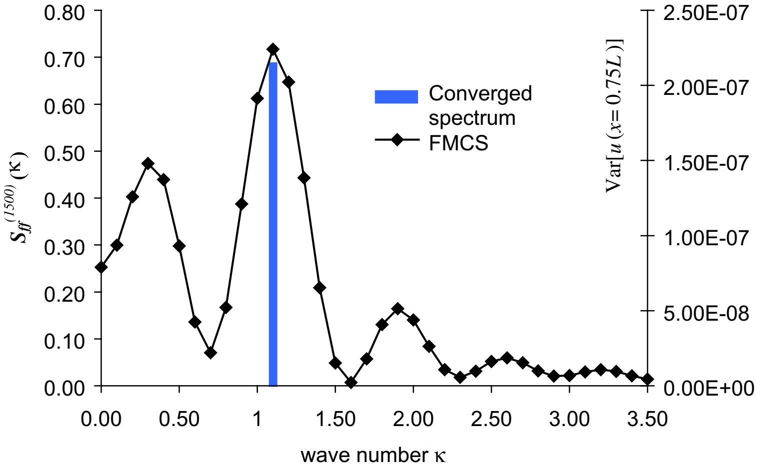

Fig. 5. Converged power spectrum of $f(x)$ determined using the brute-force optimization procedure for the response displacement at $x = 0.75L$ of the beam in Fig. 2 with LC2, and $\text{Var}[u(x = 0.75L)]_\kappa$ established by computing VRF(x,κ) through FMCS and then multiplying by σ_{ff}^2.

at six different iteration steps in this figure (specifically: 0, 25, 50, 100, 500, and 1500). It can be observed that the optimization procedure converges after approximately 1500 iterations, while for the next 1000 iterations (up to 2500) the spectrum shown in Fig. 4(f) remains unchanged having all its power concentrated at the first band of the discretized wave number domain. This is the power spectrum of a random sinusoid with $\kappa = 0$. The corresponding maximum variance of the response displacement at $x = L/2$ is computed as: $\max\{\text{Var}[u(x = L/2)]\} = 2.8 \times 10^{-6}\,\text{m}^2$. The corresponding upper bound for Var[$u(x)$] obtained using fast Monte Carlo simulation (FMCS) to compute VRF(x,κ) and subsequent application of Eq. (10) can be established from Fig. 3 (it is straightforward to show that the "brute-force MCS" curve in Fig. 3 is equivalent to using FMCS to compute VRF(x,κ) and then multiplying by σ_{ff}^2). Fig. 3 indicates an identical upper bound equal to 2.8×10^{-6} m^2, occurring also for a random sinusoid at $\kappa = 0$.

Fig. 5 shows results for the case of the beam in Fig. 2 with LC2. The response displacement is considered now at $x = 0.75L$. As for the previous case (Fig. 4), the brute-force optimization procedure converges again after approximately 1,500 iterations, while for the next 1000 iterations (up to 2500) the spectrum remains unchanged having all its power concentrated at a single band of the discretized wave number domain. This is the power spectrum of a random sinusoid with $\kappa = 1.1$. Note that Fig. 5 displays only $S_{ff}^{(1500)}(\kappa)$ which is indicated as a single bar at $\kappa = 1.1$. The corresponding maximum variance of the response displacement at $x = 0.75L$ is computed as: $\max\{\text{Var}[u(x = 0.75L)]\} = 2.2 \times 10^{-7}\,\text{m}^2$. Fig. 5 displays also a curve denoted "FMCS" which is the variance of the response displacement at $x = 0.75L$ when stochastic field $f(x)$ is a random sinusoid with all its power concentrated at wave number κ. This curve is computed by determining VRF(x,κ) through FMCS and then multiplying by σ_{ff}^2. The values of this curve as a function of the wave number κ of each random sinusoid are denoted by $\text{Var}[u(x = 0.75L)]_\kappa$. The maximum value of this curve indicates an identical upper bound as with the brute-force optimization approach (equal to 2.2×10^{-7} m^2), occurring also for a random sinusoid at the same wave number $\kappa = 1.1$.

The above two examples provide some numerical validation of the conjecture postulating the existence of the integral form for Var[$u(x)$] shown in Eq. (22) for statically indeterminate beams. An immediate consequence of this conjecture is that realizable upper bounds of the response displacement variance can be computed using Eq. (10), after the VRF(x, κ) is estimated using the fast Monte Carlo simulation (FMCS) approach described earlier. In the remaining part of this paper, this will be the approach followed to establish $\mathrm{Var}[u(x)]_\kappa$ as a function of the wave number κ of the random sinusoid, and to eventually determine a realizable upper bound of the response displacement variance as the maximum among the values of $\mathrm{Var}[u(x)]_\kappa$ computed over a wide range of wave numbers. It is pointed out that such FMCS-based computations are computationally very efficient as mentioned earlier.

3.3. Important note regarding the conjectured integral form for Var[u(x)] in Eq. (22)

The conjectured integral form in Eq. (22) for the response displacement variance of the statically indeterminate beam is the same as that suggested in previous studies (e.g. [5–7]) with one notable exception. In the past, $S_{ff}(\kappa)$ represented the power spectrum of a stochastic field $f(x)$ modeling the variation of the elastic modulus around its mean value, while in the current study $f(x)$ models the variation of the inverse of the elastic modulus. We believe that although both interpretations of $f(x)$ are essentially based on conjectures, the current one based on the inverse of the elastic modulus is a more meaningful one from the physical point of view.

4. Bound generating fields

As mentioned earlier, the upper bounds of the response displacement variance for both statically determinate and indeterminate beams are obtained when the stochastic field $f(x)$ modeling the inverse of the elastic modulus becomes a random sinusoid with power concentrated at wave number $\kappa^{\max}$ where the variability response function takes its maximum value (refer to Eq. (10) that is exact for statically determinate beams and conjectured for statically indeterminate beams). Consequently, the following expression can be written for the inverse of the elastic modulus that produces the upper bounds:

$$\frac{1}{E(x)} = F_0[1 + f(x)] = F_0[1 + \sqrt{2}\sigma_{ff}\cos(\kappa^{\max}x + \phi)], \tag{26}$$

where ϕ is a random phase angle uniformly distributed in the range $[0, 2\pi]$. A new stochastic field $f^*(x)$ modeling the elastic modulus (rather than its inverse) can now be defined for this case that produces the upper bounds

$$E(x) = \frac{1}{F_0}\frac{1}{[1 + f(x)]} = E_0[1 + f^*(x)], \tag{27}$$

where E_0 is the mean value of the elastic modulus which is related to F_0 via

$$E_0 = \frac{1}{F_0}\varepsilon\left[\frac{1}{(1 + f(x))}\right], \tag{28}$$

$f^*(x)$ is a zero-mean, homogeneous stochastic field related to $f(x)$ through the following relationship:

$$f^*(x) = \frac{1 - \varepsilon\left[\frac{1}{(1 + f(x))}\right](1 + f(x))}{\varepsilon\left[\frac{1}{(1 + f(x))}\right](1 + f(x))} \tag{29}$$

Eq. (29) indicates that stochastic field $f^*(x)$ producing the upper bound of the response displacement variance is an associated field according to the definition given in [4] and [5]. According to this definition, an associated field is a non-Gaussian stochastic field obtained by a nonlinear transformation of an underlying random sinusoid (in this case $f(x)$). Since stochastic field $f^*(x)$ produces realizable upper bounds, it will be called a Bound Generating Field (BGF).

As the relationship $f^* = G(f)$ is a decreasing one, the probability density function of $f^*(x)$ (denoted by $p_{f^*}(s^*)$) can be computed from that of the random sinusoid $f(x)$ (denoted by $p_f(s)$ and shown in Eq. (13)) as follows:

$$p_{f^*}(s^*) = \left|\frac{\mathrm{d}f}{\mathrm{d}f^*}\right| p_f(s) = \frac{1}{\left\{\varepsilon\left[\frac{1}{1+f(x)}\right](1+s^*)^2\right\}} \frac{1}{\pi}\left[2\sigma_{ff}^2 - \left\{\frac{1-\varepsilon\left[\frac{1}{1+f(x)}\right](1+s^*)}{\varepsilon\left[\frac{1}{1+f(x)}\right](1+s^*)}\right\}^2\right]^{-1/2}. \tag{30}$$

The probability density function of stochastic field $f^*(x)$ in Eq. (30) is plotted schematically in Fig. 6. From this figure, it can be observed that the zero-mean $p_{f^*}(s^*)$ is a U-shaped distribution with a lower limit f_0 having infinite probability mass and an upper limit f_1 having significant (but finite) probability mass. The shape of this distribution is similar, but not identical, to that of a random sinusoid that has a symmetric U-shaped beta distribution (Eq. (13)). As can be readily observed in Eq. (30), $p_{f^*}(s^*)$ is fully defined from the standard deviation σ_{ff} of the underlying random sinusoid $f(x)$. Table 1 presents the values of the lower and upper limits of $f^*(x)$ (f_0^* and f_1^* respectively) as a function of σ_{ff}, while Fig. 7 plots $\sigma_{f^*f^*}$ as a function of σ_{ff}. Table 1 and Fig. 7 indicate that as σ_{ff} approaches the value of $1/\sqrt{2}$, the lower limit f_0^* approaches the value of -1, the upper limit f_1^* approaches infinity, the standard deviation $\sigma_{f^*f^*}$ tends to infinity, and $p_{f^*}(s^*)$ becomes asymptotically an L-shaped distribution. In the following, $p_{f^*}(s^*)$ will be called bound probability distribution (BPD), as it is the pdf associated with the bound generating field (BGF) $f^*(x)$.

Sample functions of stochastic field $f^*(x)$ can be easily obtained from generated realizations of the random sinusoid $f(x)$ using Eq. (29). Fig. 8 displays such sample functions of $f^*(x)$ for four different values of the standard deviation σ_{ff} and a representative value of the wave number where all the power of the random sinusoid $f(x)$ is concentrated (in this case $\bar{\kappa} = 0.5$). From this figure, it can be observed that the distribution of the values of the modulus of elasticity along the length of the beam consists of zones of weak material that can be interpreted as areas that approach the behavior of a hinge, followed by zones of strong material

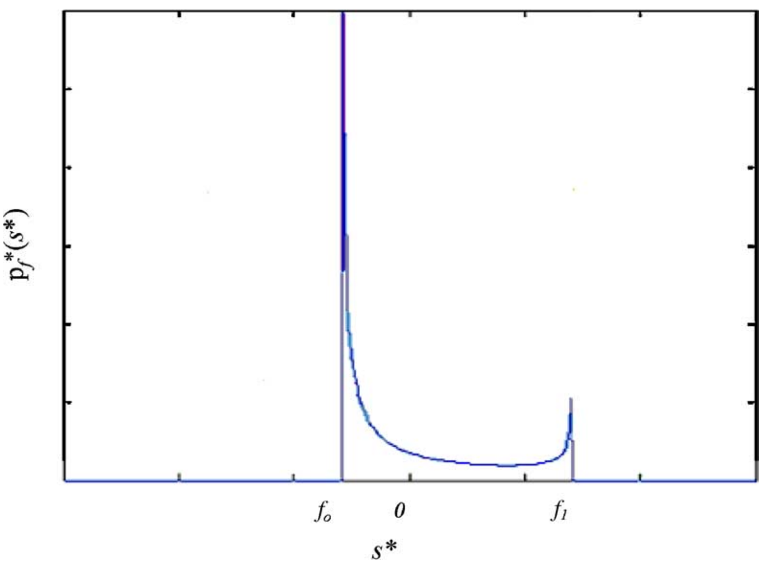

Fig. 6. Schematic plot of bound probability density function of bound generating field $f^*(x)$.

Table 1
Lower and upper limits of stochastic field $f^*(x)$ for various values of the standard deviation σ_{ff} of stochastic field $f(x)$ (which is a random sinusoid)

σ_{ff}	0.1	0.2	0.3	0.4	0.5	0.6	0.7	0.7071
Lower limit f_0^*	−0.1327	−0.2522	−0.3645	−0.4734	−0.5859	−0.714	−0.929	−0.998
Upper limit f_1^*	0.1529	0.3377	0.5722	0.8985	1.4138	2.492	13.072	→∞

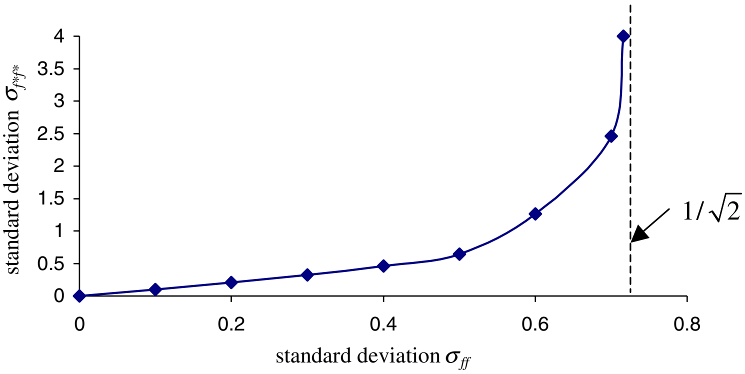

Fig. 7. Standard deviation $\sigma_{f^*f^*}$ of stochastic field $f^*(x)$ as a function of the standard deviation σ_{ff} of stochastic field $f(x)$ (which is a random sinusoid).

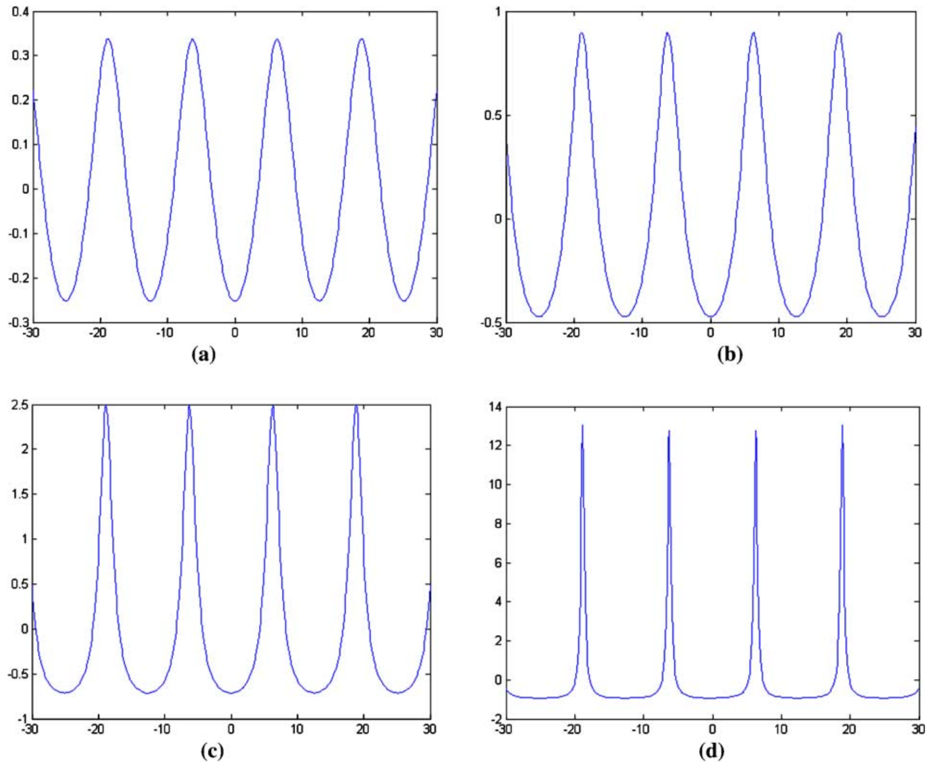

Fig. 8. Sample realizations of the bound generating field $f^*(x)$ for $\overline{\kappa} = 0.5$ and (a) $\sigma_{ff} = 0.2$, (b) $\sigma_{ff} = 0.4$, (c) $\sigma_{ff} = 0.6$ and (d) $\sigma_{ff} = 0.7$.

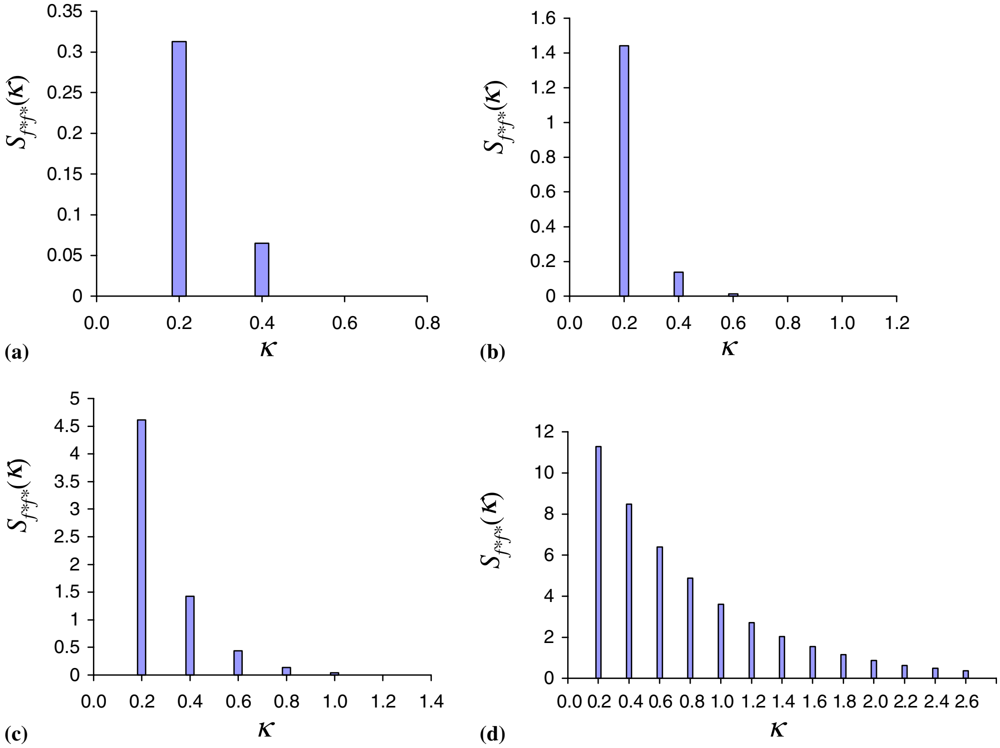

Fig. 9. Power spectral densities of the bound generating field $f^*(x)$ for $\overline{\kappa} = 0.2$ and (a) $\sigma_{ff} = 0.2$, (b) $\sigma_{ff} = 0.4$, (c) $\sigma_{ff} = 0.6$ and (d) $\sigma_{ff} = 0.7$.

that approach the behavior of a rigid body. Consequently, the following simple interpretation of the underlying physical mechanism that is responsible for creating the upper bound for the system's response variability can be established: the sequence of alternating "hinge-type zones" (responsible for the largest displacement responses) and "rigid zones" (responsible for the smallest displacement responses), leads to the maximum variability on the response displacement.

The spectral density function of the generated sample functions of stochastic field $f^*(x)$ can then be estimated numerically using the following expression:

$$S_{f^*f^*}(\kappa) = \frac{1}{2\pi L_x}\left|\int_0^{L_x} f^*(x)\mathrm{e}^{-\mathrm{i}\kappa x}\,\mathrm{d}x\right|^2, \tag{31}$$

where L_x is the length of the sample function. Using Eq. (31), the spectral density functions of $f^*(x)$ are computed and displayed in Fig. 9 for the same four values of σ_{ff} and a new representative value of the wave number where all the power of the random sinusoid $f(x)$ is concentrated (in this case $\overline{\kappa} = 0.2$). As can be seen in this figure, $S_{f^*f^*}(\kappa)$ has its power concentrated at a series of discrete wave numbers that are integer multiples of the basic wave number where all the power of the random sinusoid $f(x)$ is concentrated (in this case $\overline{\kappa} = 0.2$). The dominant peak of $S_{f^*f^*}(\kappa)$ occurs at this basic wave number $\overline{\kappa} = 0.2$.

4.1. Three alternative ways to perform fast Monte Carlo simulation

Eq. (29) indicates that when random field $f(x)$ modeling the inverse of the elastic modulus is a random sinusoid, random field $f^*(x)$ modeling the elastic modulus can be fully determined, i.e. a sample function of

$f^*(x)$ can be computed from a given sample function of $f(x)$. Consequently, there are essentially three alternative ways to perform the fast Monte Carlo simulation to estimate $\mathrm{Var}[u(x)]_{\overline{\kappa}}$:

(1) By generating sample functions of $f(x)$ (in this case a random sinusoid) and then using a closed-form analytic expression for the response displacement (e.g. Eq. (2) or (15)). This approach will be called $ANA - f(x)$.
(2) By generating sample functions of $f(x)$ (in this case a random sinusoid), computing the corresponding sample functions of $f^*(x)$ using Eq. (29), and then using a closed-form analytic expression for the response displacement. This approach will be called $ANA—f^*(x)$.
(3) By generating sample functions of $f(x)$ (in this case a random sinusoid), computing the corresponding sample functions of $f^*(x)$ using Eq. (29), and then using a deterministic finite element code to estimate the response displacement. This approach will be called $FEM—f^*(x)$.

It is obvious that the third approach is not requiring the existence of a closed-form analytic expression for the response displacement. All three approaches provide identical estimates of $\mathrm{Var}[u(x)]_{\overline{\kappa}}$ (and consequently of $\mathrm{VRF}(x, \overline{\kappa})$ too).

5. Numerical results

5.1. Statically determinate beam

Consider the statically determinate beam of length $L = 10\,\mathrm{m}$ shown in Fig. 1, carrying a uniformly distributed load $Q_0 = 1000\,\mathrm{N/m}$ and a concentrated moment $M_0 = 10{,}000\,\mathrm{N \cdot m}$ at its free end. The loads are assumed to be static and deterministic. The inverse of the elastic modulus of the beam is assumed to vary randomly along its length according to Eq. (1) with $F_0 = 8 \times 10^{-9}\,{}^2/\mathrm{N}$ and $I = 0.1\ \mathrm{m}^4$.

Spectral- and probability-distribution-free upper bounds on the response variability of this beam can be established using only the value of the standard deviation σ_{ff} of stochastic field $f(x)$ modeling the inverse of the elastic modulus. These bounds are computed using Eq. (10), following the evaluation of the maximum value of $\mathrm{VRF}(x,\kappa)$ from the closed-form expression in Eq. (8). This approach of determining the upper bounds using the analytic expression of the variability response function in Eq. (8) will be denoted by VRF in the following. There are also three alternative ways of determining the maximum value of $\mathrm{VRF}(x, \kappa)$ by estimating the variability response function numerically. This is accomplished through Eq. (24) and computing $\mathrm{Var}[u(x)]_{\kappa}$ using the three different ways described earlier in section "Three alternative

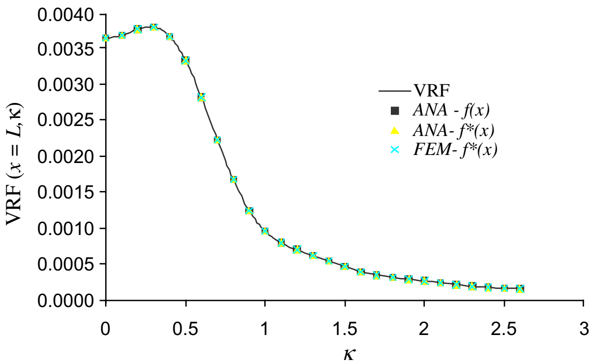

Fig. 10. Variability response function of statically determinate beam.

ways to perform fast Monte Carlo simulation'' (denoted by *ANA—f*(*x*), *ANA—f**(*x*) and *FEM—f**(*x*)). Fig. 10 displays the computed values of VRF($x = L, \kappa$) obtained using the four aforementioned approaches. The four curves are practically identical with only negligible differences due to numerical approximations. The three fast Monte Carlo simulation curves (*ANA—f*(*x*), *ANA—f**(*x*) and *FEM—f**(*x*)) are computed using a standard deviation of $\sigma_{ff} = 0.2$. It should be mentioned that identical results should be obtained for VRF($x = L, \kappa$) for any other value of $\sigma_{ff} < 1/\sqrt{2}$. Fig. 11 presents plots for Var[$u(x = L)$]$_\kappa$ that are obtained as the product of VRF($x = L, \kappa$) (curve in Fig. 10) times σ_{ff}^2. Four curves are provided corresponding to four different values of σ_{ff}^2. The upper bound for the variance of $u(x = L)$ is then simply established as the maximum value of each of the Var[$u(x = L)$]$_\kappa$ curves in Fig. 11. From the way the Var[$u(x = L)$]$_\kappa$ curves are determined, all their maximum values occur at the same wave number ($\kappa^{\max} = 0.3$ in this case). It is worthwhile noting that in this case $\kappa^{\max}$ is different from zero.

5.2. Statically indeterminate beam

Consider now the statically indeterminate beam of length $L = 10$ m shown in Fig. 2, carrying a uniformly distributed load $Q_0 = 1000$ N/m and a concentrated moment $M_0 = 10{,}000$ N m at its right end (please note that this concentrated moment is not indicated in Fig. 2). The loads are assumed again to be static and deterministic. The inverse of the elastic modulus of the beam is assumed to vary randomly along its length according to Eq. (1) with $F_0 = 8 \times 10^{-9}$ m^2/N and $I = 0.1$ m^4.

Spectral- and probability-distribution-free upper bounds on the response variability of this beam can be established using only the value of σ_{ff}. These bounds are computed again using Eq. (10), but now VRF(x, κ) can only be estimated numerically using the three alternative approaches: *ANA—f*(*x*), *ANA—f**(*x*) and *FEM—f**(*x*). Fig. 12 displays the computed values of VRF($x = L/2, \kappa$) obtained using these three approaches. The three curves are practically identical with only negligible differences due to numerical approximations. All three curves are computed using $\sigma_{ff} = 0.2$ (identical results should be obtained for any other value of $\sigma_{ff} < 1/\sqrt{2}$). Fig. 13 presents plots for VRF($x = L/2, \kappa$) that are obtained as the product of VRF($x = L/2, \kappa$) (curve in Fig. 12) times σ_{ff}^2. Four curves are provided again corresponding to four different values of σ_{ff}^2.

The upper bound for the variance of $u(x = L/2)$ is then simply established as the maximum value of each of the Var[$u(x = L/2)$]$_\kappa$ curves in Fig. 12. From the way the Var[$u(x = L/2)$]$_\kappa$ curves are determined, all their

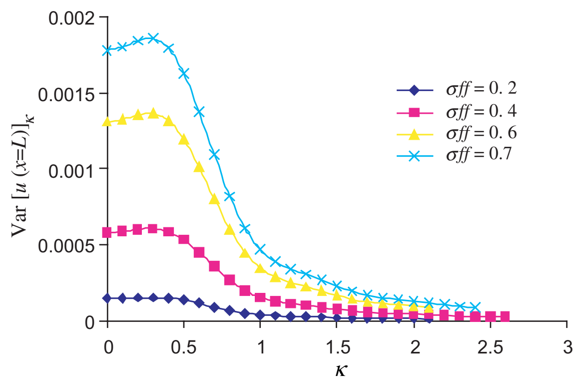

Fig. 11. Variance of response displacement of statically determinate beam when the stochastic field *f*(*x*) modeling the inverse of the elastic modulus is a random sinusoid with all its power concentrated at wave number κ. Each curve is obtained as the product of VRF($x = L, \kappa$) (curve in Fig. 10) times σ_{ff}^2. The maximum value of each curve is the spectral- and probability-distribution-free upper bound.

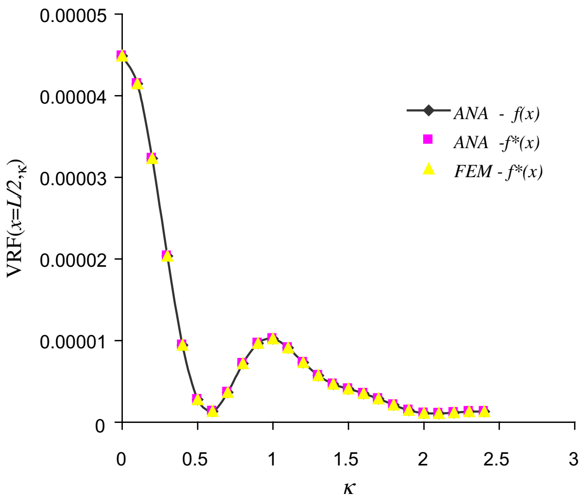

Fig. 12. Variability response function of statically indeterminate beam.

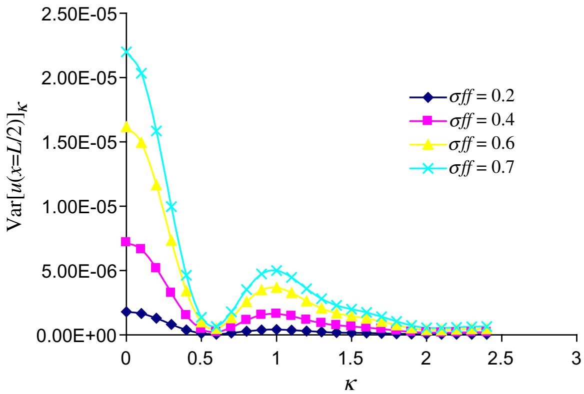

Fig. 13. Variance of response displacement of statically indeterminate beam when the stochastic field $f(x)$ modeling the inverse of the elastic modulus is a random sinusoid with all its power concentrated at wave number κ. Each curve is obtained as the product of VRF($x = L/2,\kappa$) (curve in Fig. 12) times σ_{ff}^2. The maximum value of each curve is the spectral- and probability-distribution-free upper bound.

maximum values occur at the same wave number ($\kappa^{\max} = 0$ in this case). It is worthwhile noting that although in this case $\kappa^{\max}$ is equal to zero, there are numerous other cases of statically indeterminate beam configurations where the maximum values occur at $\kappa^{\max} \neq 0$.

6. Conclusions

Spectral- and probability-distribution-free upper bounds on the response variability of both statically determinate and indeterminate beams were established in the present paper based on exact closed-form analytic expressions derived for the variance of the response displacement. A conjecture had to be made in the case of statically indeterminate beams in order to establish these bounds.

The upper bounds proposed in this study are called spectral- and probability-distribution-free because they require knowledge of only the variance of the stochastic field modeling the inverse of the elastic modulus. Such bounds are realizable in the sense that it is possible to fully determine the probabilistic characteristics (spectral density function and marginal probability distribution function) of the stochastic field (modeling the inverse of the elastic modulus) that produces them. Furthermore, it is possible to fully determine also the corresponding stochastic field modeling the elastic modulus that produces these bounds.

It was shown that the upper bounds can also be computed numerically using a so-called fast Monte Carlo simulation (FMCS) procedure, taking advantage of the fact that the bounds are obtained when the stochastic field modeling the inverse of the elastic modulus becomes a random sinusoid. The FMCS procedure is not requiring a closed-form analytic expression for the response displacement, making this approach much more general.

Finally, it is recognized that the existence of such bounds in the statically indeterminate case is based on a conjecture and remains to be shown in a rigorous mathematical way. It is reminded that the conjecture was supported through an argument postulating the existence of the integral form in Eq. (23) and through a brute-force optimization procedure providing numerical validation. In addition, the quality of the upper bounds established in this study in terms of their usefulness and admissibility in real life applications should be tested in the future in the context of their impact on the design of real structures. The extension of the proposed methodology to more complex real world structures is a subject of future research.

Acknowledgement

This work was supported by the National Science Foundation under Grant # CMS-01-15901, with Dr. Peter Chang as Program Director.

References

[1] G. Deodatis, M. Shinozuka, Bounds of response variability of stochastic systems, J. Engrg. Mech. 115 (11) (1989) 2543–2563.
[2] G. Deodatis, Weighted integral method I: stochastic stiffness matrix, J. Engrg. Mech. 117 (8) (1991) 1851–1864.
[3] G. Deodatis, M. Shinozuka, Weighted integral method II: response variability and reliability, J. Engrg. Mech. 117 (8) (1991) 1865–1877.
[4] G. Deodatis, L. Graham, R. Micaletti, A hierarchy of upper bounds on the response of stochastic systems with large variation of their properties: random variable case, Prob. Engrg. Mech. 18 (4) (2003) 349–364.
[5] G. Deodatis, L. Graham, R. Micaletti, A hierarchy of upper bounds on the response of stochastic systems with large variation of their properties: random field case, Prob. Engrg. Mech. 18 (4) (2003) 365–375.
[6] L. Graham, G. Deodatis, Weighted integral method and variability response functions for stochastic plate bending problems, Struct. Safety 20 (1998) 167–188.
[7] L. Graham, G. Deodatis, Stochastic response and random eigenvalues of structural systems with multiple uncertain material and geometric properties, Prob. Engrg. Mech. 16 (1) (2000) 11–29.
[8] P.S. Koutsourelakis, G. Deodatis, Simulation of binary random fields: application to random media, in: Proceedings of 9th International Conference on Applications of Statistics and Probability in Civil Engineering, July 6–9, San Francisco, CA, 2003.
[9] M. Shinozuka, Structural response variability, J. Engrg. Mech. 113 (6) (1987) 825–842.
[10] F.J. Wall, G. Deodatis, Variability response functions of stochastic plane stress/strain problems, J. Engrg. Mech. 120 (9) (1994) 1963–1982.
[11] I. Elishakoff, Y. Ren, M. Shinozuka, Some exact solutions for the bending of beams with spatially stochastic stiffness, Int. J. Solids Struct. 32 (16) (1995) 2315–2327.